Single-molecule assay reveals strand switching and enhanced processivity of UvrD

Marie-Noëlle Dessinges*†, Timothée Lionnet*†‡, Xu Guang Xi‡§, David Bensimon*†, and Vincent Croquette*†

*Laboratoire de Physique Statistique, Ecole Normale Supérieure, Unité Mixte de Recherche 8550, Centre National de la Recherche Scientifique, 24 Rue Lhomond, 75231 Paris Cedex 05, France; †Departement de Biologie, Ecole Normale Supérieure, 46 Rue d'Ulm, 75231 Paris Cedex 05, France; and §Laboratoire de Biotechnologies et Pharmacologie Génétique Appliquée, Ecole Normale Supérieure Cachan, Unité Mixte de Recherche 8113, Centre National de la Recherche Scientifique, 61 Avenue du Président Wilson, 94235 Paris Cedex, France

Edited by Kiyoshi Mizuuchi, National Institutes of Health, Rockville, MD, and approved February 2, 2004 (received for review October 17, 2003)

DNA helicases are enzymes capable of unwinding double-stranded DNA (dsDNA) to provide the single-stranded DNA template required in many biological processes. Among these, UvrD, an essential DNA repair enzyme, has been shown to unwind dsDNA while moving 3′-5′ on one strand. Here, we use a single-molecule manipulation technique to monitor real-time changes in extension of a single, stretched, nicked dsDNA substrate as it is unwound by a single enzyme. This technique offers a means for measuring the rate, lifetime, and processivity of the enzymatic complex as a function of ATP, and for estimating the helicase step size. Strikingly, we observe a feature not seen in bulk assays: unwinding is preferentially followed by a slow, enzyme-translocation-limited rezipping of the separated strands rather than by dissociation of the enzymatic complex followed by quick rehybridization of the DNA strands. We address the mechanism underlying this phenomenon and propose a fully characterized model in which UvrD switches strands and translocates backwards on the other strand, allowing the DNA to reanneal in its wake.

helicase | DNA replication | DNA repair | magnetic tweezers

Although helicases are essential molecular motors, their precise mechanism is only partially known. These motors translocate along DNA while stripping off one strand of the double helix (1, 2). Whereas a large number of helicases involved in DNA repair and recombination are either monomeric or dimeric, replicative helicases typically form processive, hexameric entities surrounding one or both strands. The process of separating the two strands of DNA is often described as the translocation of the enzyme on one strand, which defines the directionality of the process, whereas the displacement of the other strand is accomplished actively, if the helicase melts the base pairs, or, passively, if the helicase moves forward as the bases transiently unpair. Observing the activity of a single helicase unwinding a double helix yields valuable information on the enzymatic dynamics, as has been the case for other molecular motors such as kinesin and myosin (3).

UvrD (720 aa, molecular mass = 82 kDa), a member of the helicase SF1 superfamily (which includes PcrA and Rep), plays a crucial role in nucleotide excision repair and methyl-directed mismatch repair (4–8) and is required for the replication of several plasmids (9). It has been shown to initiate unwinding from a 3′ end single-stranded DNA (ssDNA) tail, a gap, or a nick and to translocate along ssDNA in a 3′-5′ direction (10–12). The purpose of this study is to investigate the mechanochemistry of UvrD-catalyzed DNA unwinding at the single-molecule level, yielding more direct insight into its enzymatic activity by avoiding the inherent averaging of bulk assays. We present real-time measurements of the unwinding rate, lifetime, and number of base pairs unwound, as well as an estimate of the step size. In addition, we observe that an unwinding event can be followed by an enzyme-translocation-limited rehybridization of the opened strands. We propose that this rehybridization is due to the enzyme switching strands, and we fully characterize the rate constants of this model by using our data.

Materials and Methods

Substrate Preparation. Charomid DNA (13), a gift from O. Hyrien (Laboratoire de la Génétique Moléculaire, Ecole Normale Supérieure), is cut with *Apa*I and *Kpn*I to produce a 11-kbp fragment. Eight hundred base pairs of DNA fragments multiply labeled with either biotin or digoxigenin are synthesized by PCR from the multiple cloning site of the Bluescript vector and cut respectively with *Apa*I and *Kpn*I. The 11-kbp fragment is differentially end-labeled by ligating to each extremity the complementary 800-bp fragment. DNA is first mixed with streptavidin magnetic beads (diameter 4.5 μm, Dynal, Great Neck, NY) and incubated for 10 min. The bead–DNA construct is then incubated on an antidigoxigenin-coated glass surface previously incubated with tRNA (Sigma) to reduce nonspecific interactions. After the beads have sedimented, we use a gentle flow to eliminate untethered beads from the capillary.

Protein Purification. A full coding region of UvrD gene is prepared by PCR by using *Escherichia coli* chromosome DNA. The 2.2-kbp PCR product is cloned into pGEM-T easy vector, and the sequence of this insert is shown to be identical to the UvrD gene sequence (14). The UvrD gene is amplified again by PCR and then digested with *Nde*I and *Xho*I, and the 2.1-kb fragment is gel-purified and subcloned into *Nde*I/*Xho*I sites of the vector PET-15b. The constructed plasmid is further sequenced by MWG Biotech (Ebersberg, Germany). His-6-tagged *E. coli* UvrD helicase is expressed from pET-15b expression plasmid in *E. coli* strain BL21 (DE3) (15). The overexpressed protein is purified under native conditions by using chromatography on Ni^{2+}-nitrilotriacetic acid columns (Qiagen, Valencia, CA), followed by FPLC size exclusion chromatography (Superdex 200, Pharmacia) and an ion-exchange chromatography (DEAE Sephadex A-50). Based on Sypro Orange-stained SDS/PAGE and electrospray mass spectrometry analyses, the purity of the UvrD preparation is determined to be >95%.

Single-Molecule Assay Conditions. Experiments are performed at 25°C in 20 mM Tris·HCl, 25 mM NaCl, 3 mM $MgCl_2$, 0.1 mM EDTA, and 1 mM DTT. ATP (Amersham Pharmacia) is added to the final concentration indicated. The very low DNA concentration is impossible to determine accurately. We estimate that it is smaller than the DNA concentration in the bead–DNA solution, and greater than the concentration of beads tethered by a DNA molecule in the capillary, i.e., that 10^{-18} M < [DNA] < 10^{-15} M.

ATPase Bulk Assay. The ATPase activity is determined in a bulk assay by a measure of the radioactive $^{32}P_i$ liberated during

This paper was submitted directly (Track II) to the PNAS office.

Abbreviations: ssDNA, single-stranded DNA; dsDNA, double-stranded DNA; MM, Michaelis-Menten.

‡To whom correspondence should be addressed. E-mail: Timothee.Lionnet@lps.ens.fr or Xi@lbpa.ens-cachan.fr.

hydrolysis (16). Briefly, the measurement is carried out at 25°C in a reaction mixture containing 1.5 μM (nucleotide) heat-denatured *Hin*dIII-cut pGEM-7Zf linear DNA at the indicated concentration of ATP. The reactions are initiated by the addition of UvrD helicase into a 100-μl reaction mixture and stopped by pipetting 80 μl aliquots from the reaction mixture every 30 s into a hydrochloric solution of ammonium molybdate. The liberated radioactive $^{32}P_i$ is extracted with a solution of 2-butanol-benzene-acetone-ammonium molybdate (750:750:15:1) saturated with water. An aliquot of the organic phase is counted in 6 ml of Aquasol.

Single-Molecule Measurements. Bead tracking and force measurements are performed on an inverted microscope as described (17). Briefly, a DNA molecule bound at one end to a glass surface and at the other to a small magnetic bead is stretched by the magnetic field gradient generated by small magnets placed above the sample. By optically tracking at video rate (25 Hz) the diffraction pattern around the bead, we measure its 3D position (x, y, and z). The uncertainties in the position are due to Brownian fluctuations. In the z direction, they reach the value of $\approx$1 nm^2·Hz^{-1} (at a force $F = 35$ pN and for frequencies $f > 2$ Hz). The molecule extension L is obtained from the average mean height $L = \langle z \rangle$. To eliminate variations in $\langle z \rangle$ due to microscope drift, differential tracking with a second bead glued to the surface is performed. The bead's transverse fluctuations $\langle \delta x^2 \rangle$ allow for a determination of the stretching force by means of the equipartition theorem: $F = k_B T \langle z \rangle / \langle \delta x^2 \rangle$ ($k_B T = 4$ pN·nm at 25°C) (17). Here, F is measured with a 15% accuracy. Results are obtained at $F = 35$ pN except as otherwise mentioned. The magnets create a force field that varies on a millimeter scale. Because the tethered magnetic bead moves only by a few micrometers, the variation of F during an unwinding experiment is negligible. We detect nicked molecules by rotating the magnets and identifying the molecules that do not supercoil (18). We perform measurements only on singly nicked molecules, which we select by briefly stretching above 65 pN to melt the duplex (19). Molecules with more than one nick will break (if both strands are nicked), or lose a piece of ssDNA (if one strand is multiply nicked). Because the majority of molecules tested neither broke nor lost a significant piece of DNA, we conclude that the sample consists of molecules nicked at a single (but random) position.

Data Processing. The determination of the helicase unwinding rate requires measuring the elongation vs. time $L(t)$. The number of base pairs unwound is given by: $N(t) = [L(t) - L(0)]/\delta L(F)$, where $\delta L(F)$ is the change in extension between double-stranded DNA (dsDNA) and ssDNA per base pair at force F. The local velocity v_i of the helicase is determined as described (19) by fitting the data in an extension burst $L(t)$ to a polygon $\{L_i, t_i\}$ of $i = 1, \ldots, M$ vertices, and computing the local slope $v_i = (L_i - L_{i-1})/(t_i - t_{i-1})$. Data at $F = 35$ pN were collected over nine DNA molecules (436 bursts) at [ATP] = 500 μM. Data at 15, 40, 80, and 200 μM ATP were collected over respectively 76, 76, 99, and 175 bursts.

Results

Monitoring Helicase Activity at the Level of a Single Enzymatic Complex. To monitor UvrD activity at the single-complex level, we specifically anchor a singly nicked dsDNA molecule at one end to a magnetic bead and at the other to a glass surface (Fig. 1*A* and *Materials and Methods*). Magnets placed above the sample control the vertical force F stretching the molecule (19). The difference in extension between stretched ssDNA and dsDNA allows us to monitor the unwinding activity (see *Materials and Methods*). At high force, ssDNA extends more than dsDNA ($\delta L(F) \approx 0.135$ nm/bp at $F = 35$ pN) so that unwinding

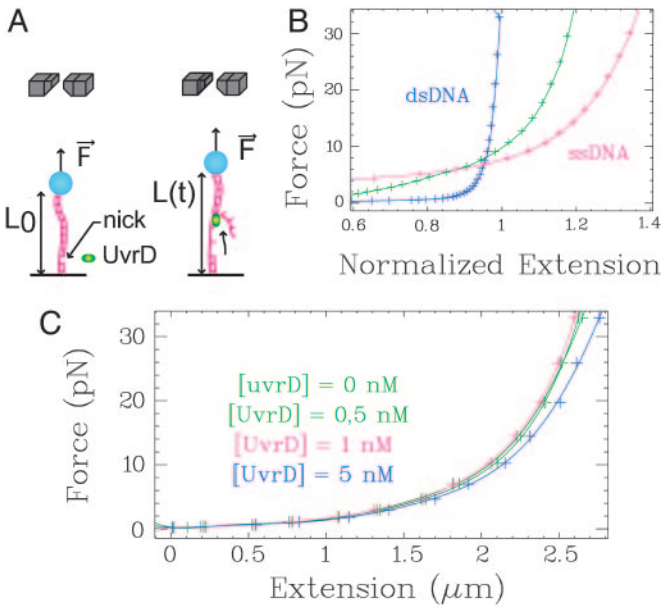

Fig. 1. Experimental set-up. (*A*) Magnets (gray) exert an adjustable, constant force F on a bead tethered to the surface by a nicked DNA molecule. (*B*) Extension of a stretched dsDNA (blue), ssDNA (red), and a partially ds-ssDNA molecule (green) (normalized to the crystallographic length of the dsDNA). (*C*) Force–extension curves of ssDNA in the presence of increasing concentrations of UvrD ([ATP] = 500 μM). Within our working conditions ([UvrD] $\leq$ 1 nM), the change in extension of ssDNA is negligible.

events result in an increase in $L(t)$ (Fig. 1*B*). Below 5 pN, ssDNA is shorter than dsDNA, leading to a decrease in extension on unwinding. Therefore, the helicase works against the force below 5 pN and with the force above 5 pN. The binding of UvrD on the freed ssDNA does not affect its length within the range of concentrations used in the experiments in single enzymatic complex conditions ([UvrD] ≤ 1 nM $\ll K_d \approx 10$ nM; refs. 20 and 21 and Fig. 1*C*). For [UvrD] < 1 nM (and $F > 30$ pN), the extension signal displays isolated bursts (Fig. 2*A*). They consist of a regular increase in extension as the DNA is unwound, followed by a much faster decrease when the enzyme dissociates from its substrate, thus allowing the strands to rehybridize quickly. These "UH" bursts (unwinding-rehybridization), are not observed in the absence of UvrD, ATP, or Mg^{2+} or when selecting a molecule having no nick (Fig. 7, which is published as supporting information on the PNAS web site). Because the timespan of an unwinding burst is 10- to 100-fold smaller than the time between two bursts, it is extremely unlikely that unwinding results from the simultaneous activity of multiple enzymatic complexes (18). Moreover, the simultaneous action of two complexes displays a characteristic doubling of the unwinding rate (sometimes observed at higher enzyme concentrations, Fig. 2*D*). From the slope of the increase in extension, we can deduce the unwinding rate, v_U; from the burst height, we deduce the number of base pairs unwound, N_U; and from its duration, we deduce the unwinding lifetime, τ_U (see Fig. 2 *A* and *B* for definitions). From the slope of the decreasing part of the burst, we can deduce the average DNA rehybridization rate: $\langle v_H \rangle \approx$ 2,300 bp/s, which is ATP-independent and similar to the rehybridization rate after a brief stretch above 65 pN of a nicked DNA molecule (see *Materials and Methods*). In all cases, unwinding proceeds uniformly and processively with no detectable pauses.

Under the same conditions, we observe another type of burst (Fig. 2*B*), displaying a similar increase in extension due to unwinding, but followed by much slower reannealing. These

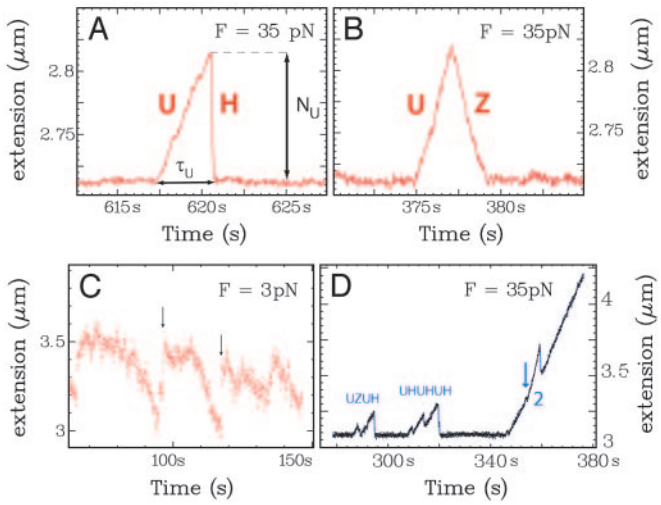

Fig. 2. Typical unwinding signals. At high forces, the extension of ssDNA is longer than dsDNA, and unwinding is observed as an increase in the molecule's extension (*A* and *B*): $F = 35$ pN; [UvrD] = 0.25 nM; [ATP] = 500 μM. (*A*) UH event (unwinding-rehybridization). (*B*) UZ event (unwinding-rezipping). (*C*) UvrD activity at $F = 3$ pN and [UvrD] = 50 nM. Unwinding is observed at low forces ($F < 5$ pN) as a decrease in the DNA's extension. Quick rehybridization (arrows) is still observed on dissociation of the enzyme. (*D*) Helicase activity observed at [UvrD] = 2 nM ([ATP] = 500 μM). At this UvrD concentration, there is enough binding of the enzyme to the ssDNA generated during an unwinding event to allow for successive rounds of unwinding, resulting in burst bunching. Notice also the simultaneous unwinding by two helicases. The arrow indicates when a second helicase has become active, doubling the unwinding rate. When one of the helicases dissociates, the rate of unwinding resumes its initial value.

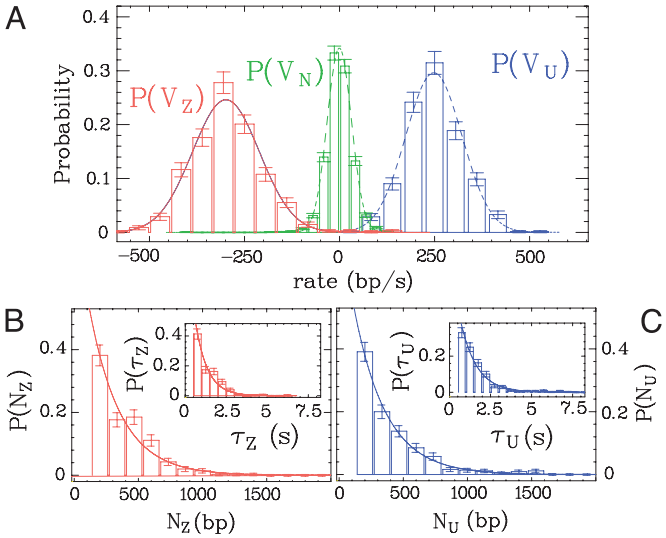

Fig. 3. Distributions of the unwinding and rezipping rates, lifetimes, and numbers of base pairs unwound at [ATP] = 500 μM. (*A*) The unwinding rate v_U (blue curve), rezipping rate v_Z (red curve), and the experimental noise v_N between bursts (green curve) are fitted to Gaussian distributions (dashed curves) of mean value $\langle v_U \rangle = 248 \pm 3$ bp/s, $\langle v_Z \rangle \approx -298 \pm 3$ bp/s and $\langle v_N \rangle = -0.6 \pm 0.7$ bp/s and SD $\sigma(v_U) = 74$ bp/s, $\sigma(v_Z) = 88$ bp/s, and $\sigma(v_N) = 32$ bp/s. (*B*) Number of base pairs rezipped N_Z and rezipping lifetime τ_Z (*Inset*), fitted to Poisson distributions with mean value $\langle N_Z \rangle = 234 \pm 13$ bp and $\langle \tau_Z \rangle = 0.73 \pm 0.05$ s. UH and UZ bursts give similar values of $\langle v_U \rangle$, $\langle N_U \rangle$, and $\langle \tau_U \rangle$. (*C*) Number of base pairs unwound N_U and unwinding lifetime τ_U (*Inset*), fitted to Poisson distributions with mean value $\langle N_U \rangle = 240 \pm 14$ bp and $\langle \tau_U \rangle = 0.98 \pm 0.05$ s. The error bars on the histograms represent the statistical error in the bins.

events are denoted UZ: unwinding-rezipping. The rezipping rate v_Z varies similarly with ATP concentration as the unwinding rate v_U (see below). The decrease in the length of the molecule observed during rezipping events never goes below the dsDNA baseline length (although we sometimes observe more complicated burst patterns, e.g., UZU or UZH). These features suggest that the rezipping events consist of an enzyme translocation-limited closing of the two strands opened during unwinding. Another helicase, RecQ, was similarly studied and did not display any rezipping activity (data not shown).

We define the rezipping rate v_Z, lifetime τ_Z, and extent N_Z as, respectively, the slope, duration, and height of the rezipping part of the burst. We observe that at [ATP] = 500 μM, the mean unwinding and rezipping rates v_U and v_Z follow Gaussian distributions of mean value $\langle v_U \rangle = 248 \pm 3$ bp/s and $\langle v_Z \rangle = -298 \pm 3$ bp/s and SDs $\sigma(v_U) = 74$ bp/s and $\sigma(v_Z) = 88$ bp/s, more than twice the width of the experimental noise distribution (Fig. 3*A*). This increased variability of the rate could result from sequence dependence of the rate or from enzyme to enzyme variability. The distribution of the number of base pairs unwound N_U and rezipped N_Z as well as the unwinding and rezipping lifetimes τ_U and τ_Z follow Poisson distributions of mean value $\langle N_U \rangle = 240 \pm 14$ bp, $\langle N_Z \rangle = 234 \pm 13$ bp, $\langle \tau_U \rangle = 0.98 \pm 0.05$ s, and $\langle \tau_Z \rangle = 0.73 \pm 0.05$ (Fig. 3 *B* and *C*).

Helicase Activity at Various ATP Concentrations. By varying the ATP concentration, we observe that the Michaelis-Menten (MM) kinetics obtained in a bulk ATPase assay [$\langle V_{ATP} \rangle = k_{cat}[ATP]/(K_M + [ATP])$, with $k_{cat} = 95 \pm 3\ s^{-1}$ and $K_M = 53 \pm 4$ μM] agree with the ATP dependence of v_U and v_Z (K_M constrained to 53 μM, $v_U^{max} = 275$ bp/s, and $v_Z^{max} = -333$ bp/s, Fig. 4*A*). This agreement constitutes a good control for our results. However, that the measured value of k_{cat} is subject to the usual caveats of bulk measurements, namely the possible presence of inactive enzymes, means that the quoted value of that k_{cat} is a lower bound. The unwinding lifetime $\langle \tau_U \rangle = 0.83 \pm 0.08$ s is ATP-independent (Fig. 4*D*), a feature also observed for RecBCD (22, 23). This result suggests that UvrD's dissociation rate from ssDNA is not affected by its ATPase activity, even though the latter is stimulated by ssDNA binding. It is consistent with these observations that $\langle N_U \rangle$ displays a MM kinetics similar to $\langle v_U \rangle$ (K_M constrained to 53 μM, and $N_U^{max} = 255$ bp, Fig. 4*C*) with $N_U^{max} \approx v_U^{max} \langle \tau_U \rangle$. The rate v_Z follows the same MM kinetics as $\langle v_U \rangle$, with $\langle |v_Z| / v_U \rangle = 1.17 \pm 0.03$ over the whole ATP concentration range (Fig. 4 *A* and *B*). This finding demonstrates that these slow rezipping (Z) events are limited by the ATP-dependent enzyme translocation, in contrast with the fast rehybridization events (H), whose rate is ATP independent.

Helicase Activity at Smaller Forces and Higher Enzymatic Concentration. At low concentrations of enzyme ([UvrD] < 1 nM), we observe isolated unwinding bursts only when $F > 30$ pN (Fig. 5*A*). However, by increasing the concentration of UvrD to 50 nM ($> K_d = 10$ nM), we can observe unwinding at very low forces (Fig. 2*C*). In this regime, individual events cannot be distinguished. This event bunching is due to the increased stability of the unwound strands against reannealing resulting from their coating by UvrD. It is therefore impossible to measure the number of base pairs unwound per event N_U at such concentrations. However, the rate of unwinding is well defined and is very similar to the high force rate ($\approx 200 \pm 60$ bp/s at [ATP] = 500 μM and [UvrD] = 50 nM). This rate is difficult to compute accurately because the kinetics of UvrD binding to the ssDNA generated in the wake of the complex is unknown. Thus, the calibration factor $\delta L(F)$ cannot be determined. It is bound between its value for bare ssDNA and its equilibrium value at the studied UvrD concentration, which differ by 15%. It is never-

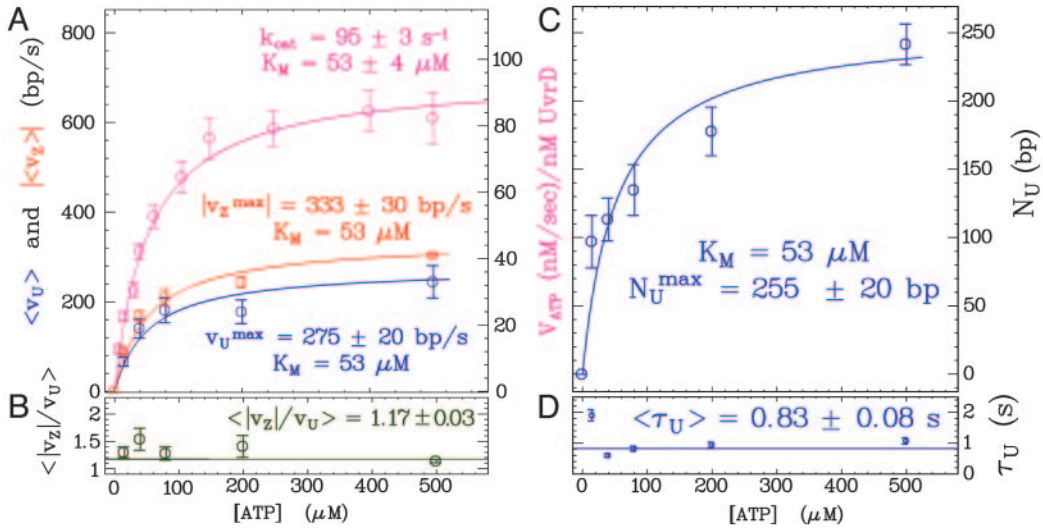

Fig. 4. Rates, unwinding and rezipping extents and lifetimes as a function of ATP. (*A*) UvrD single-molecule unwinding rate $\langle v_U \rangle$ (blue), rezipping rate $\langle v_Z \rangle$ (red), and bulk ATP hydrolysis rate V_{ATP} (magenta) are fitted to the same MM kinetics. (*B*) The ratio $\langle |v_Z|/v_U \rangle$ is ATP-independent. The error on $|v_z|/v_u$ is only statistical. Because the value at 500 μM results from 288 points against typically 50 for the others, the associated error is much smaller and dominates the global mean value. (*C*) The mean unwinding extent N_U follows the same MM kinetics as the unwinding rate. (*D*) The unwinding lifetime $\langle \tau_U \rangle$ is ATP-independent. Each point is the average over histograms obtained on typically five DNA molecules.

theless remarkable that v_U varies by <20% between $F = 3$ and 35 pN because the enzyme works energetically downhill at high forces but uphill below 5 pN (recall that, for F < 5 pN, the molecule shortens as it is unwound; Fig. 1*C*). This result implies that our rate measurements on a single helicase at high forces can be extrapolated to zero force. Because the force does not affect the velocity, the enzyme rate-limiting step is associated neither with the enzyme's displacement nor with DNA opening.

Stochastic Stepping of UvrD Along Its Substrate Increases the Noise Level. We have performed a Fourier analysis of the noise associated with the measurement of the molecule's extension. When a helicase is not actively unwinding the studied molecule, its extension remains constant ($v_U = 0$). The fluctuations in extension are solely due to the Brownian fluctuations of the bead and are characterized by a frequency-independent spectrum (for frequencies $f < 30$ Hz at $F = 35$ pN). In contrast, during a burst of unwinding activity, the mean square fluctuations in extension $\delta L^2 = (L(t) - \langle v_U \rangle t)^2$ are enhanced by the stochastic stepping of the enzyme. We use this increased noise to estimate the helicase step size δz, i.e., the number of bases opened per enzymatic cycle (24). In Fourier space, this extra noise increases at low frequencies as A/f^2 (Fig. 6). The magnitude of A is related to the enzymatic rate $\langle v_U \rangle$ and step size δz by $A = \delta z \langle v_U \rangle / 2\pi^2$, assuming that the duration of enzymatic cycles follows a Poisson distribution, i.e., that a single biochemical step limits the enzymatic turnover (25, 26). If there are two or more steps with comparable rate constants that limit the enzymatic turnover, then the model predicts that δz is a lower bound for the step size. The more rate-limiting steps, the more regular the cycle and the greater the step size required to produce a given amplitude of stochastic noise. Our data yield $\delta z = 0.8 \pm 0.15$ nm corresponding to 6 ± 1.5 bp unwound per cycle, a value consistent with stop-flow estimates of ≈4–5 bp (27). A similar analysis of the rezipping data yields the same step size.

Because of smaller processivity at low [ATP], we estimate δz only at saturating [ATP]. In principle, we cannot rule out that the step hereby estimated actually consists of a series of sequential smaller steps separated from the next series by a pause. The MM kinetics for the rate would require these pauses to be ATP dependent, which is very unlikely. The value of δz might also be

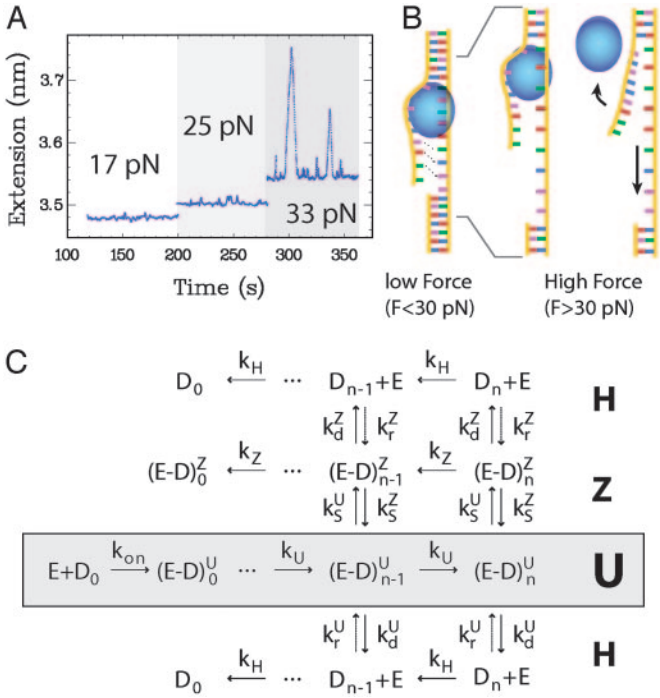

Fig. 5. (*A*) Single helicase activity is observed only above 30 pN. ([UvrD] ≈ 0.25 nM, [ATP] = 500 μM, a low-pass filter at 1 Hz was applied to the time trace for clarity). (*B*) Above 30 pN (*Right*), the separated strands behind the helicase are slightly mismatched in the stressed strand as compared with the free one. This mismatch inhibits rehybridization as long as the enzyme binds to the fork and thus hinders nucleation. When UvrD dissociates, reannealing can proceed from the seed provided by the fork. Below 30 pN, the kinetic barrier preventing reannealing behind the helicase is lowered so the strands are able to rehybridize behind the helicase, preventing any observation of an unwinding signal. (*C*) Kinetic scheme of UvrD activity. E refers to free enzyme, D_n to free DNA with $n \cdot \delta z$ bp unwound. $(E\text{-}D)_n^U$ and $(E\text{-}D)_n^Z$ denote the UvrD–DNA complexes in U and Z states respectively, with $n \cdot \delta z$ bp unwound. Dashed arrows indicate events that are due to resumption of the enzymatic activity by the same enzyme or by another one bound to the ssDNA fraction. Note that k_H corresponds to the rehybridization of 1 bp, in contrast with k_u and k_z, which correspond to steps of δz bp.

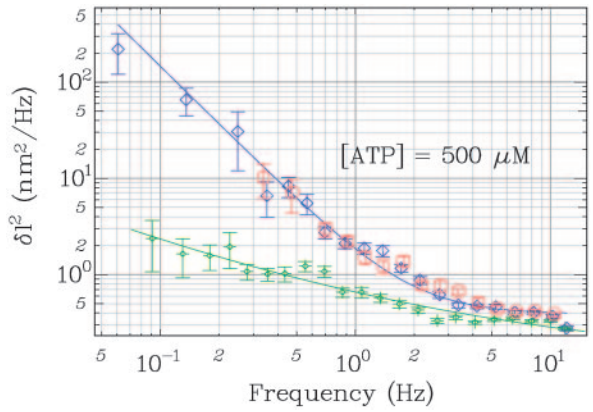

Fig. 6. The average power spectra of unwinding (blue, $n = 438$) and rezipping activity (red, $n = 291$) are fitted to $\delta l^2 = \delta z \langle v_U \rangle / 2\pi^2 f^2 + b$, leading to the same step size $\delta z = 6 \pm 1.5$ bp. Experimental noise between activity bursts (green, $n = 424$) is shown for comparison.

overestimated due to variability of the rate with the sequence. Our method relies essentially on the same statistical principles used in a quenched flow estimate (27) and thus shares the same drawbacks.

Discussion

Strand Switching. To address the mechanism underlying the observations of UZ bursts, we can imagine three models. First, the enzyme might be able to switch polarity on the same strand from 3′-5′ to 5′-3′ in the course of its translocation. Second, when the complex dissociates, rehybridization of the two strands could be hindered by another enzyme that happens to be translocating 3′-5′ on the complementary strand. Third, the enzyme might switch strands in the course of unwinding and end up translocating on the complementary strand. Such a strand-switching mechanism could involve a partial or total release of the enzyme from its substrate. The first hypothesis is incompatible with previous results demonstrating that UvrD translocation occurs only with a 3′-5′ directionality (10). The second one is highly unlikely: at [UvrD] = K_d = 10 nM, the mean distance between two helicases bound to ssDNA is of the order of 20 nt because, at saturation, one monomer occupies 10 nt (28). When we reduce the UvrD concentration to our working conditions (0.25 nM), the mean distance l between monomers reaches $l \approx 20{\cdot}10/0.25 = 800$ nt. This distance is larger than the average number of base pairs unwound: $\langle N_U \rangle \approx 240$ bp. Therefore, the probability for the fork to be blocked by an enzyme translocating on the displaced strand is very small. We deduce that UvrD switches strands in the course of its translocation, actively unwinding dsDNA as it moves 3′ to 5′ on one strand, and allowing passive rehybridization of the separated strands in its wake after it switches to moving 3′ to 5′ on the other (see details of the model in Fig. 5*C*). This strand-switching pathway is preferred to dissociation because 65% of the bursts observed at [ATP] = 500 μM are of this type. After a strand-switching transition, the enzyme can dissociate (UZH burst), switch strands a second time (UZU burst), or translocate back to its entry point. At this point, if the enzyme is bound to the nicked unstretched strand, it will dissociate (UZ burst with the Z part going back to the baseline as in Fig. 2*B*). Alternatively, if the enzyme is translocating back to its entry point on the intact stretched strand, it might possibly move further. This type of event produces a trace identical to the one resulting from a UZU event in which the second strand-switching transition (Z back to U) occurs right at the nick position (as in the first burst of Fig. 2*D*, UZUH).

Table 1. Definitions and values (at [ATP] = 500 μM) of the rate constants of the proposed kinetic pathway

Reaction	Rate constant, s^{-1}
Unwinding	$k_U = 41.3 \pm 4$
Strand switching from U state	$k_s^U = 0.67 \pm 0.07$
Dissociation from U state	$k_d^U = 0.36 \pm 0.04$
Rezipping	$k_Z = 47.1 \pm 5$
Strand switching from Z state	$k_s^Z = 0.37 \pm 0.2$
Dissociation from Z state	$k_d^Z = 0.034 \pm 0.02$
Rehybridization	$k_H = 2{,}300 \pm 200$
Rescue from H to U state	k_r^U –
Rescue from H to Z state	k_r^Z –

The biological advantage of strand switching is not clear yet, but it is possible to form a conjecture. Recent experiments demonstrated that Srs2 (the ortholog of UvrD in Eukaryotes), in addition to its helicase activity, plays a regulatory role in homologous recombination. This regulation is mediated by the displacement of Rad51 recombinase from ssDNA (29, 30). Other helicases from T4 bacteriophage (gp41 and Dda) were also shown to displace streptavidin from biotinylated single-stranded oligonucleotides (31). If UvrD had to regulate the binding of proteins to DNA, displacing proteins along one strand and then along its complementary one might be an efficient mechanism to clear the DNA. In the following, we propose a new kinetic scheme to describe strand switching and fully characterize it by using our data.

Kinetic Scheme of UvrD Activity. Our single-molecule experiments allow us to deduce all of the rate constants defined in the reaction pathway (Fig. 5*C*) at [ATP] = 500 μM (Table 1). The rate constants k_u and k_z are simply computed from the rates of unwinding and rezipping by using the estimate for the step size: $k_u = \langle v_U \rangle / \delta z = 41.3 \pm 4\ s^{-1}$, and similarly $k_z = \langle v_Z \rangle / \delta z = 47.1 \pm 5\ s^{-1}$. The value of k_u is approximately three times larger than quenched flow estimates (27, 32), a significant but not unusual difference when comparing single-molecule and bulk assays. The causes of this discrepancy still remain to be fully understood.

Let p_s^u or p_d^u (p_s^z or p_d^z) be the probabilities per cycle that the enzyme switches strands or dissociates in the course of an unwinding (rezipping) event. The processivity p^u, defined as the probability per cycle to perform one enzymatic step forward (i.e., neither switching strand nor dissociating) is related to p_s^u and p_d^u by $p^u = 1 - p_s^u - p_d^u$. But p^u is also related to the mean number of enzymatic cycles performed during a burst of activity: $\langle N \rangle = \langle N_U \rangle / \delta z = 240/6 = 40 \pm 13$ cycles, so $p^u = \exp(-1/\langle N \rangle) = 0.975 \pm 0.009$. Therefore, $p_s^u + p_d^u = 1 - p^u = 0.025 \pm 0.009$. On the other hand, the ratio of UZ to UH events (288/155) must be equal to the ratio of probabilities $p_s^u/p_d^u = 288/155 = 1.86$. We thus deduce $p_s^u = 0.016 \pm 0.005$ and $p_d^u = 0.009 \pm 0.003$. Because the probabilities p_s^u and p_d^u are related to the rate constants through $p_s^u = k_s^u/(k_s^u + k_d^u + k_u)$ and $p_d^u = k_d^u/(k_s^u + k_d^u + k_u)$, we deduce $k_d^u = 0.36 \pm 0.16\ s^{-1}$ and $k_s^u = 0.67 \pm 0.30\ s^{-1}$.

A similar analysis can be done for the rate constants on the rezipping (Z) pathway. It shows that the probability distribution of the number of base pairs rezipped (N_z) must be proportional to $\exp[-N_z(p_s^u + p_d^u + p_s^z + p_d^z)]$. Fitting the data for N_z to an exponential distribution yields $p_s^u + p_d^u + p_s^z + p_d^z = 0.033 \pm 0.01$. Using the previous values of p_s^u and p_d^u, we deduce that $p_s^z + p_d^z = 0.008 \pm 0.004$. From the ratio of UZH to UZU events (3/33), we obtain $p_d^z/p_s^z = 3/33 = 0.091 \pm 0.07$. This result allows us to compute k_s^z and k_d^z as previously done for k_s^u and k_d^u: $k_s^z = 0.37 \pm 0.2\ s^{-1}$ and $k_d^z = 0.034 \pm 0.02\ s^{-1}$.

The small difference between v_U and v_Z shows that the rate of UvrD on DNA is only slightly affected by the enzyme having to

open the strands or by the fork closing in its wake (Fig. 4*B*). These results directly suggest that the unwinding mechanism is active. Because we expect the velocity of UvrD on ssDNA to obey $v_U \leq v_{ssDNA} \leq v_Z$, our results imply that $v_{ssDNA} \approx 270$ bp/s. We observe that the step size is the same for the U and Z events. Because $v_u^{max} \approx v_z^{max}$, it is reasonable to assume that the enzymatic efficiencies for unwinding, rezipping, and ssDNA translocation are similar. Thus, we estimate by using the bulk ATPase assay that UvrD consumes $\approx k_{cat}/v_u^{max} = 0.35$ ATP/bp unwound. However, bulk ATPase consumption may not result solely from the enzyme's translocation. Therefore, the observed k_{cat} may not reflect the ATP hydrolysis rate during translocation. Moreover, this estimate must be taken with caution because it is prone to the usual errors inherent in bulk estimates (presence of inactive enzymes, etc).

The Stretching Force Affects DNA Rehybridization in the Wake of the Complex. All helicase assays require a means to prevent the two DNA strands from rehybridizing in the wake of the enzymatic complex. Although in bulk assays this is usually done by using single-strand binding proteins, in our single-molecule experiment, the force F stretching the DNA substrate presents a very efficient way to solve this reannealing problem. In our assay, for the strands to rehybridize in the wake of the enzyme, a thermal fluctuation must provide the activation energy ΔE_a required to match the separated unloaded strand with the stretched one. We estimate that activation energy to be: $\Delta E_a \approx N \cdot F \cdot \delta L(F)$, where $N \approx 10$ (33) is the number of nucleotides covered by the helicase footprint and $\delta L(F)$ is the overextension per base pair of stretched ssDNA in comparison with dsDNA (assuming that the distance between bases bound by the helicase is the same as in dsDNA). At $F = 35$ pN, $\delta L(F) = 0.135$ nm, so that $\Delta E_a \approx 10\ k_BT$, which reduces the rehybridization frequency by more than four orders of magnitude. The stretching force combined with the enzyme's footprint thus create a kinetic barrier that prevents reannealing during the timespan of an unwinding burst. This finding explains why we observe unwinding events only when $F >$ 30 pN (Fig. 5 *A* and *B*). As the helicase dissociates, reannealing can proceed from the fork through successive matching of single base pairs. The kinetic barrier is thus drastically reduced, and rehybridization is fast.

At low forces ($F < 30$ pN), the tension is not sufficient to build a kinetic barrier that prevents reannealing. In this regime, it is possible to generate a kinetic barrier as usually done in bulk experiments, i.e. by coating the separated single strands with single-strand binding protein or with UvrD itself, which has a strong affinity for ssDNA ($k_d \approx 10$ nM for UvrD). Indeed, we are able to observe unwinding activity at $F = 3$ pN if we increase UvrD concentration above 10 nM (Fig. 2*C*).

However, at high enzymatic concentrations, the observed unwinding activity is not simply related to the UvrD concentration (because many enzymes may be bound and inactive). To overcome this limitation, stop-flow experiments have studied the activity of helicases prebound to short oligomers (20–30 bps long) and quickly mixed with ATP (27). In that situation, the helicase itself sets a kinetic barrier that hinders DNA reannealing, favoring the complete separation of the two DNA strands.

The use of specific experimental conditions to prevent reannealing of the separated strands is the most likely reason for the differences between single-molecule results and bulk data, namely the observation of single-molecule activity at subnanomolar enzymatic concentrations where none was reported in bulk assays, and the shift between the average number of base pairs unwound in the single-molecule assay ($N_u^{max} = 265$ bp) compared with previous single-turnover experiments (45 bp; ref. 27). The force-generated lowering of the energy required to melt the DNA might also be another processivity-increasing factor.

Although at this stage we cannot draw definite conclusions from these measurements about the oligomeric state of the complex, our data show that, under certain conditions, UvrD could be much more processive than assumed from its bulk *in vitro* behavior. It is also possible that the stretching force, besides preventing reannealing of the separated strands, helps the enzyme to plow through the DNA. This effect does not influence significantly the rate of unwinding but could affect the enzymatic processivity.

We thank T. M. Lohman and A. M. Pyle for critical discussions on the manuscript and G. Charvin and O. A. Saleh for a careful reading of the manuscript. We are grateful to J. F. Allemand for his help in improving the experimental set-up and to H. Q. Xu for his assistance in protein purification. This work was supported by grants from Association pour la Recherche sur le Cancer, Centre National de la Recherche Scientifique, Ecole Normale Supérieure, the Universities of Paris VI and Paris VII, and the European Mol Switch Project (IST-2001-38036).

1. Delagoutte, E. & Hippel, P. H. V. (2002) *Q. Rev. Biophys.* **35,** 431–478.
2. Delagoutte, E. & Hippel, P. H. V. (2003) *Q. Rev. Biophys.* **36,** 1–69.
3. Hua, W., Chung, J. & Gelles, J. (2002) *Science* **295,** 844–848.
4. Lohman, T. M. & Bjornson, K. P. (1996) *Annu. Rev. Biochem.* **65,** 169–214.
5. West, S. C. (1996) *Cell* **86,** 177–180.
6. Soultanas, P. & Wigley, D. (2001) *Trends Biochem. Sci.* **26,** 47–54.
7. Sancar, A. (1994) *Science* **266,** 1954–1956.
8. Yamaguchi, M., Dao, V. & Modrich, P. (1998) *J. Biol. Chem.* **273,** 9197–9201.
9. Bruand, C. & Ehrlich, S. D. (2000) *Mol. Microbiol.* **35,** 204–210.
10. Matson, S. W. (1986) *J. Biol. Chem.* **261,** 10169–10175.
11. Runyon, G. T. & Lohman, T. M. (1989) *J. Biol. Chem.* **264,** 17502–17512.
12. Brosh, R. M. J. & Matson, S. W. (1997) *J. Biol. Chem.* **272,** 572–579.
13. Saito, I. & Stark, G. R. (1986) *Proc. Natl. Acad. Sci. USA* **83,** 8664–8668.
14. Yamamoto, Y., Ogawa, T., Shinagawa, H., Matsuo, H. & Ogawa, H. (1986) *J. Biochem (Tokyo)* **99,** 1579–1590.
15. Xu, H. Q., Deprez, E., Zhang, A. H., Tauc, P., Ladjimi, M. M., Brochon, J. C., Auclair, C. & Xi, X. G. (2003) *J. Biol. Chem.* **278,** 34925–34933.
16. Avron, M. (1960) *Biochim. Biophys. Acta* **40,** 257–261.
17. Strick, T. R., Allemand, J. F., Bensimon, D. & Bensimon, A. (1996) *Science* **271,** 1835–1837.
18. Strick, T. R., Croquette, V. & Bensimon, D. (2000) *Nature* **404,** 901–904.
19. Maier, B., Bensimon, D. & Croquette, V. (2000) *Proc. Natl. Acad. Sci. USA* **97,** 12002–12007.
20. Mechanic, L. E., Latta, M. E. & Matson, S. W. (1999) *J. Bacteriol.* **181,** 2519–2526.
21. Ali, J. A., Maluf, N. K. & Lohman, T. M. (1999) *J. Mol. Biol.* **293,** 815–834.
22. Bianco, P. R., Brewer, L. R., Corzett, M., Balhorn, R., Yeh, Y., Kowalczykowski, S. C. & Baskin, R. J. (2001) *Nature* **409,** 374–378.
23. Dohoney, K. M. & Gelles, J. (2001) *Nature* **409,** 370–374.
24. Svoboda, K., Mitra, P. P. & Block, S. M. (1994) *Proc. Natl. Acad. Sci. USA* **91,** 11782–11786.
25. Charvin, G., Bensimon, D. & Croquette, V. (2002) *Single Mol.* **3,** 43–48.
26. Dekker, N. H., Rybenkov, V. V., Duguet, M., Crisona, N. J., Cozzarelli, N. R., Bensiomon, D. & Croquette, V. (2002) *Proc. Nat. Acad. Sci. USA* **99,** 12126–12131.
27. Ali, J. A. & Lohman, T. M. (1997) *Science* **275,** 377–380.
28. Maluf, N. K. & Lohman, T. M. (2003) *J. Mol. Biol.* **325,** 889–912.
29. Veaute, X., Jeusset, J., Soustelle, C., Kowalczykowski, S. C., Cam, E. L. & Fabre, F. (2003) *Nature* **423,** 309–312.
30. Krejci, L., Komen, S. V., Li, Y., Villemain, J., Reddy, M. S., Klein, H., Ellenberger, T. & Sung, P. (2003) *Nature* **423,** 305–309.
31. Morris, P. D. & Raney, K. D. (1999) *Biochemistry* **38,** 5164–5171.
32. Maluf, N. K., Fisher, C. J. & Lohman, T. M. (2003) *J. Mol. Biol.* **325,** 913–935.
33. Runyon, G. T., Wong, I. & Lohman, T. M. (1993) *Biochemistry* **32,** 602–612.